**TECHNISCHE MECHANIK**
an open access journal

journal homepage: www.ovgu.de/techmech

Tech. Mech., Vol. 43, Is. 1, (2023), 49–58

Received: 07.02.2023
Accepted: 08.02.2023
Available online: 16.02.2023

# Turbulent mixing simulation using the Hierarchical Parcel-Swapping (HiPS) model

Tommy Starick[1]*, Masoomeh Behrang[2], David O. Lignell[2], Heiko Schmidt[1], and Alan R. Kerstein[3]

[1] Brandenburg University of Technology Cottbus-Senftenberg, Institute of Transport Technology, Chair of Numerical Fluid and Gas Dynamics, Siemens-Halske-Ring 15a, 03046 Cottbus, Germany
[2] Brigham Young University, Department of Chemical Engineering, Provo, UT, 84602, USA
[3] Consultant, 72 Lomitas Road, Danville, CA, 94526, USA

**Abstract:** Turbulent mixing is an omnipresent phenomenon that permanently affects our everyday life. Mixing processes also plays an important role in many industrial applications. The full resolution of all relevant flow scales often poses a major challenge to the numerical simulation and requires a modeling of the small-scale effects. In transported Probability Density Function (PDF) methods, the simplified modeling of the molecular mixing is a known weak point. At this place, the Hierarchical Parcel-Swapping (HiPS) model developed by A.R. Kerstein [J. Stat. Phys. 153, 142-161 (2013)] represents a computationally efficient and novel turbulent mixing model. HiPS simulates the effects of turbulence on time-evolving, diffusive scalar fields. The interpretation of the diffusive scalar fields or a state space as a binary tree structure is an alternative approach compared to existing mixing models. The characteristic feature of HiPS is that every level of the tree corresponds to a specific length and time scale, which is based on turbulence inertial range scaling. The state variables only reside at the base of the tree and are understood as fluid parcels. The effects of turbulent advection are represented by stochastic swaps of sub-trees at rates determined by turbulent time scales associated with the sub-trees. The mixing of adjacent fluid parcels is done at rates consistent with the prevailing diffusion time scales. In this work, a standalone HiPS model formulation for the simulation of passive scalar mixing is detailed first. The generated scalar power spectra with forced turbulence shows the known scaling law of Kolmogorov turbulence. Furthermore, results for the PDF of the passive scalar, mean square displacement and scalar dissipation rate are shown and reveal a reasonable agreement with experimental findings. The described possibility to account for variable Schmidt number effects is an important next development step for the HiPS formulation. This enables the incorporation of differential diffusion, which represents an immense advantage compared to the established mixing models. Using a binary structure allows HiPS to satisfy a large number of criteria for a good mixing model. Considering the reduced order and associated computational efficiency, HiPS is an attractive mixing model, which can contribute to an improved representation of the molecular mixing in transported PDF methods.

**Keywords:** differential diffusion, hierarchical parcel-swapping, HiPS, mixing model, scalar mixing

## 1 Introduction

Turbulent mixing is an integral aspect of our daily life and ranges, as Sreenivasan (2019) points out, "from supernovae to cream in coffee". In nature, turbulent mixing processes are also omnipresent and play an important role, such as in combustion, meteorology and even pollutant distribution. In most cases, these flows are noted for their large range of relevant flow scales. This causes major obstacles in the numerical simulation, since the full resolution requires enormous computational resources. As Livescu et al. (2020) indicates, the numerical simulation of turbulent mixing remains as some of the most significant challenges in computational modeling. This becomes particularly significant at flows with high Reynolds and/or Schmidt numbers.
The Direct Numerical Simulation (DNS) is the most accurate method, which fully resolves all relevant length and time scales. However, this is associated with an immensely high computational effort. For that reason, DNS is not feasible for most engineering applications today and in the foreseeable future. The Reynolds-averaged Navier-Stokes equations (RANS) and the Large Eddy Simulation (LES) approach overcome this limitation by effectively removing small-scale information from the solution. LES uses a low-pass filter which reduces the computational effort in the desired way. As a result, the small-scale effects are only considered in a modeled form. Thus, the accuracy of the simulation is closely related to the quality of the applied modeling (Ferziger et al., 2020). This is particularly important for flows with a strong influence of the small-scale effects, such as wall bounded flows, reactive flows and diffusive transport processes. The same applies to the modeling of the molecular mixing/diffusion in transported Transported Probability Density Function (PDF) methods.
Transported PDF methods are widely used for the simulation of turbulent reactive flows because of the favorable treatment of the chemical source term. However, this approach requires a suitable modeling of the molecular mixing (Pope, 1985; Fox, 2003). The transport equation of the single-point joint composition PDF is given in Equation 1.

$$\frac{\partial}{\partial t}(\rho P) + \frac{\partial}{\partial x_i}(\rho u_i P) + \frac{\partial}{\partial \psi_k}(\rho S_k P) = -\frac{\partial}{\partial x_i}\left[\rho \langle u_i'' | \psi \rangle P\right] + \frac{\partial}{\partial \psi_k}\left[\rho \langle \frac{1}{\rho}\frac{\partial J_{i,k}}{\partial x_i} | \psi \rangle P\right] \tag{1}$$

* E-mail address: Tommy.Starick@b-tu.de
doi: 10.24352/UB.OVGU-2023-044

Here, $P$ stands for the Favre-averaged joint PDF of composition, $\rho$ for the mean fluid density, $u_i$ for the Favre mean fluid velocities, $u_i''$ for the velocity fluctuations, $S_k$ for the reaction rate of species $k$, $\psi$ for the composition field and $J_{i,k}$ for the molecular diffusion fluxes. All terms on the left-hand side of Equation 1 are in closed form which includes the non-linear reaction term $\frac{\partial}{\partial \psi_k}(\rho S_k P)$ (Fox, 2003). For this reason, transported PDF methods are preferably used in the simulation of reactive flows. However, the terms on the right-hand side require a modeling. For the turbulent scalar flux term $-\frac{\partial}{\partial x_i}\left[\rho\langle u_i''|\psi\rangle P\right]$, modeling is usually used, which is based on a gradient-diffusion approach $\frac{\partial}{\partial x_i}\left(\frac{\rho\mu_t}{Sc_t}\frac{\partial P}{\partial x_i}\right)$. The molecular mixing/diffusion term $\frac{\partial}{\partial \psi_k}\left[\rho\langle\frac{1}{\rho}\frac{\partial J_{i,k}}{\partial x_i}|\psi\rangle P\right]$ also requires modeling. Models for molecular mixing gain increasing importance, as this is known as one weakness of transported PDF methods (Fox, 2003).

As of today, a large number of mixing models can be found in the literature (Fox, 2003). Among all particle mixing models, the most distinctive representatives are the Interaction by Exchange with the Mean (IEM) model (Villermaux and Devillon, 1972), Linear Mean Square Estimation model (LMSE) (Dopazo and O'Brien, 1974), the Euclidean Minimum Spanning Trees (EMST) model (Subramaniam and Pope, 1998), Curl's model (Curl, 1963), and the Fokker-Planck type models (Fox, 2003).

The central challenge of these stochastic models is the representation of the mixing processes in a way that is computationally efficient, and which is able to retain a significant level of physics. The constraints for a good mixing model can be derived directly from the statistical analysis of the conditional fluctuating diffusion flux in the composition PDF transport equation, see Fox (2003); Pope (2011). Table 1 lists the constrains and desired properties for appropriate mixing models.

Tab. 1: Constraints and desired properties for a good mixing model.

| | |
|---|---|
| (I) | Scalar mean $\langle\phi\rangle$ is not directly affected by mixing |
| (II) | Mixing causes the scalar variance to decrease over time |
| (III) | Inert-scalar PDF should relax to Gaussian form in homogeneous turbulence |
| (IV) | Bounding of scalars to the so-called allowable region (e.g. positivity) |
| (V) | Mixing should be local in composition space |
| (VI) | Mixing rate should depend on scalar length scales |
| (VII) | Reynolds, Schmidt and Damköhler number dependencies should be taken into account |
| (VIII) | Differential diffusion should be respected |

In Curl's model Curl (1963), pairs of particles are randomly selected from an ensemble of particles and their compositions are fully intermixed. This method leaves the mean unchanged and ensures criterion (I) from Table 1. The mixing takes place with a frequency which is characteristic for turbulent mixing processes. As a result, the variance of inert scalars decreases over time and criterion (II) is fulfilled. However, this has the disadvantage that only discrete mixing states can be reproduced. This does not correspond to reality and criterion (IV) is only partially fulfilled. For this reason, a model modification exists (Janicka et al., 1979). Criterion (III), (V), (VI), (VII) and (VIII) are not accomplished by the Curl's model, see Fox (2003). The biggest deficiency of the model becomes apparent when considering a combustion with a thin flame front. The cold oxidizer is separated from the cold fuel by a thin, high-temperature flame sheet. The fuel must pass through the high-temperature region of the flame sheet where it is burnt before it can reach the oxidizer. In contrast, Curl's model allows fuel particles to jump into the oxidizer without reacting. This is a clear limitation of the model and causes unphysical conditions. In reality, fuel can't enter into regions of cold oxidizer without crossing the flame-sheet. This is a violation of the locality criterion (V). With a strict interpretation, the values are also outside the so-called allowable region and criterion (IV) is also not fulfilled.

An alternative to Curl's model is the IEM model (Villermaux and Devillon, 1972). In the IEM mixing model, all of the individual particles gradually and linearly evolve to an average state. The progress is controlled by a empirically determined variance reduction, see Dopazo (1979, 1994); Villermaux and Devillon (1972). Analog to Curl's model, the IEM model meets the criteria for a good mixing model on the points (I), (II) and (IV). A major disadvantage of the IEM model, analog to Curl's mixing model, is the lack of locality of the mixing process in state space (V). Another weak point is the fact that the IEM model preserves the shape of the inert-scalar PDF in homogeneous turbulence, which means that no Gaussian form can be achieved (Fox, 2003; Eswaran and Pope, 1988). Criterion (VI), (VII) and (VIII) are also not ensured by the model. Note that (Tsai and Fox, 1996) attempted to introduce length scale dependency in the IEM model by means of a spectral model for the scalar dissipation rate. However, this introduces additional modeling assumptions and complications.

In terms of the criteria in Table 1, Curl's and the IEM model have some serious limitations. In particular, the missing locality in composition space has adverse effects in some applications. The Euclidean minimum spanning tree (EMST) mixing model attempts to incorporate the locality principle into the model and seeks to address the problems encountered in flows with simultaneous mixing and reactions (Subramaniam and Pope, 1998). The EMST model is based on a mathematical construction of a minimal spanning tree, which only allows an exchange in state space between adjacent fluid elements. This requires that states within the allowable region that do not correspond to the initial condition can't be reached. As a result, criterion (IV) is violated. Like Curl's and the IEM model, criterion (I) and (II) is fulfilled by the EMST model. However, EMST does not address criterion (VI), (VII) and (VIII).

The understanding of the construction mechanism of the PDF of scalar concentrations, and of its time evolution is vital (Villermaux, 2019). As Villermaux (2019) explains, "history matters", in the sense that, stirring and diffusion being two distinctive phenomena, it is an urgent need to account for the advection of fluid parcels in the mixing modeling. Statistically, this is a multi-time or multi-point correlation for the diffusion and dispersion of individual fluid parcels (Shraiman and Siggia, 2000). Consider a key issue affecting the IEM and Curl's models: the fact that two fluid parcels that are relatively close to each other are generally in a similar chemical composition state. How can it be that these two parcels are in relatively similar chemical composition if they never

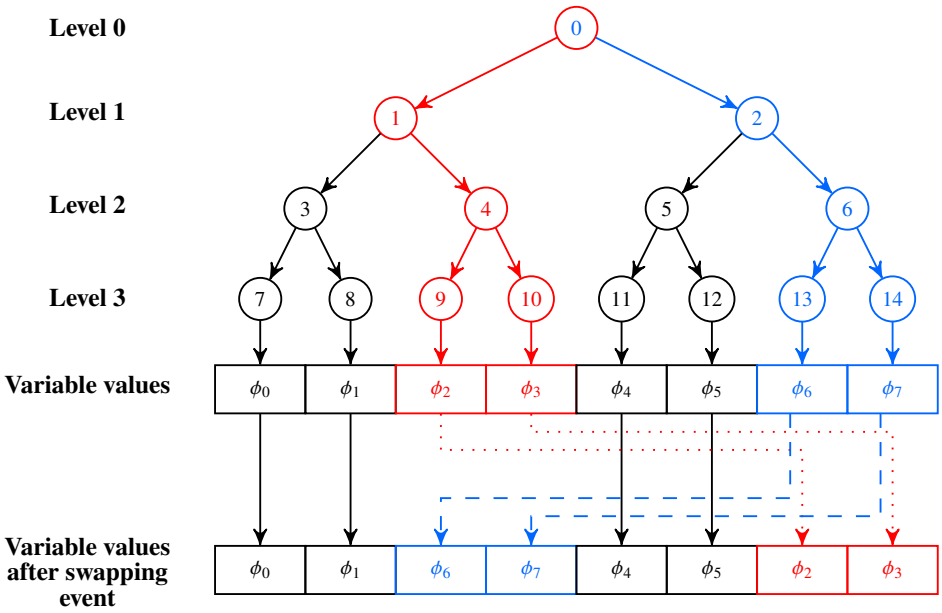


Fig. 1: Schematic illustration of a 4 level binary tree used in HiPS with a swapping event originated at node 0 with select grandchildren 4 and 6.

mixed before? Therefore, "history matters" (Villermaux, 2019; Shraiman and Siggia, 2000). However, multi-point correlations are not considered in pure composition-space stochastic mixing models such as the Curl, IEM or EMST models.

At this point, the Hierarchical Parcel Swapping (HiPS) (Kerstein, 2013) model provides an efficient mixing model which is able to incorporates the correct physics, including the dynamics of the small scales in physical space. HiPS uses a hierarchical and stochastic mechanism of swapping fluid parcels to incorporate turbulence. Unlike other purely stochastic composition-space mixing models typically used in chemical reaction engineering, HiPS incorporates, by construction, multi-point or multi-parcel correlations. This will allow the understanding of issues such as scaling laws on different regimes of scalar turbulence, structure functions, high order statistics, as well as multi-point Lagrangian statistics.

HiPS as a flexible mixing model could be incorporated in the future as a closure for higher fidelity stochastic turbulence models, hybrid stochastic and Large Eddy Simulation (LES) approaches, or as a subgrid closure in hybrid LES or Reynolds-averaged Navier–Stokes (RANS) methods (Kerstein, 2014, 2021; Glawe et al., 2018).

In the next section, the HiPS model formulation for stand-alone passive scalar simulations is detailed. In Section 3, results for passive scalar mixing with and without large-scale forcing are given. This includes the scalar power spectrum, the mean square displacement, the scalar dissipation rate and the inert-scalar PDF. Additionally, a model extension of HiPS to incorporate differential diffusion is outlined.

## 2 HiPS model

HiPS was developed as a turbulent mixing model by Kerstein (2013). The core principle of HiPS is based on the representation of effects of turbulence on time-evolving scalar fields by a binary tree structure. Interestingly, this idea of the binary tree was postulated by Obukhov (1983), according to his considerations on discrete models of turbulence. As in the discrete representation suggested by Obukhov (1983), dynamic parcels are tracked, allowing a consistent Lagrangian treatment. In HiPS, the variable values only reside at the base level of the tree, the leaf level, which is a representation of the physical solution. An exemplary representation of the HiPS binary tree with 4 levels is detailed in Figure 1. Assuming that every node has exactly 2 children, there are 8 leaves at the leaf level. The number of levels $n$ determines the number of leaves $2^{n-1}$. In Figure 1, each leaf is understood as a fluid parcel and contains a variable value $\phi_\alpha$, where $\alpha$ is an index between 0 and 7. The variable values only reside at the base of the tree. Every level $i$ of the tree is associated with a specific length scale $L_i$ and time scale $\tau_i$. The length scale of a sub-node is simply half the length of the considered node, though other so-called scale reduction factors may be used. The associated time scales follow Kolmogorov's inertial range scaling law (Kolmogorov, 1991),

$$\epsilon \sim \frac{u^2}{\tau} \sim \frac{L^2}{\tau^3}. \tag{2}$$

In Equation 2, $u$ stands for the velocity and $\epsilon$ for the dissipation rate which is taken to be constant in the inertial range. Table 2 lists the length and time scales for an $n$ level binary tree. The model rules for the representation of the effects of turbulence, which we will refer to as swapping events, are implemented by first selecting a grandparent node. A grandparent node is characterized by its children and grandchildren, such that only node 0 on level 0, as well as nodes 1 and 2 on level 1, can be considered grandparent nodes in Figure 1. The grandparent nodes are sampled in time as a Poisson process with a mean rate $\lambda_i = 2^i/\tau_i$, set by time scales

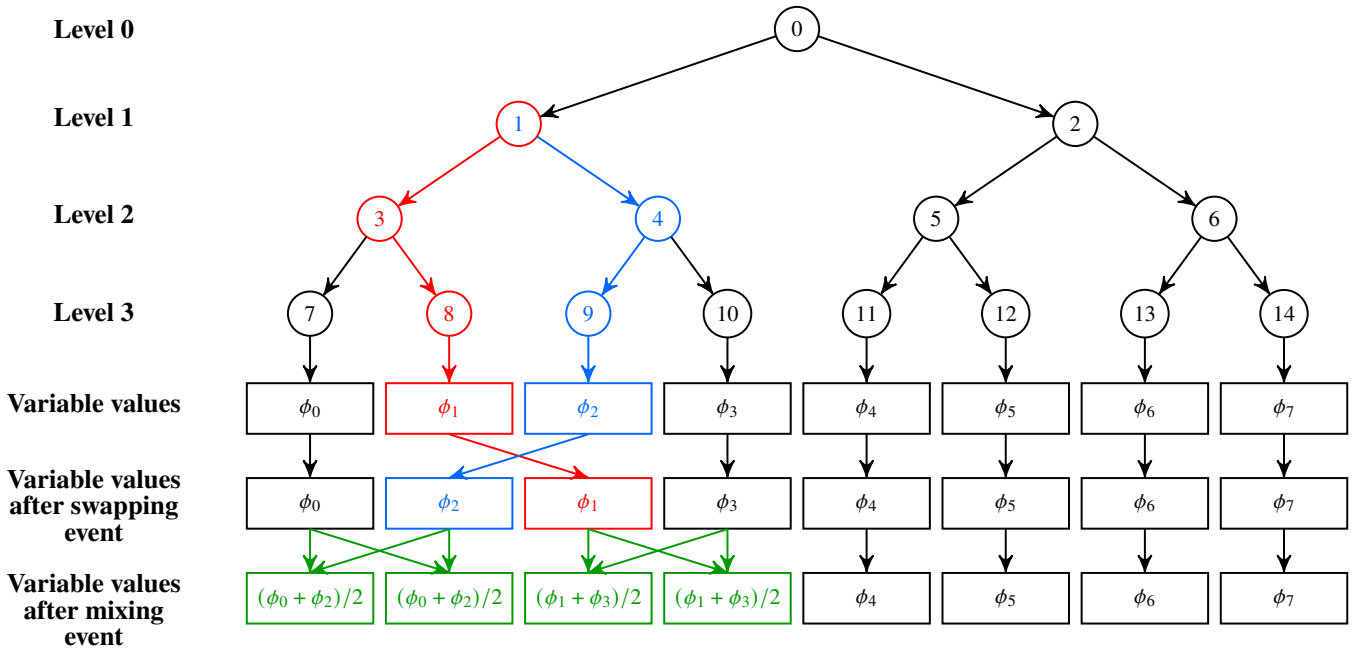


Fig. 2: Schematic illustration of a 4 level binary tree with a swapping event originated at node 1 and a subsequent mixing process. The swapping event changes the proximity of adjacent fluid parcels and requires a subsequent mixing event, which is simply done by intermixing the contents of two adjacent fluid parcels.

assigned to each level $i$ of the tree, based on Kolmogorov's inertial range scaling law (Kolmogorov, 1991),

$$\tau_i = \tau_0 \left( \frac{L_i}{L_0} \right)^{(2/3)} . \tag{3}$$

In this scaling law, $L_0$ and $\tau_0$ are the integral length and time scales assigned to level 0 of the tree, and $L_i$ and $\tau_i$ are the length and time scales of the $i$-th level of the tree. Based on Kolmogorov's hypothesis (Pope, 2011; Kolmogorov, 1991), the Reynolds number represented by the HiPS tree is defined by the tree size,

$$Re^{3/4} = \frac{L_0}{L_\eta}. \tag{4}$$

$L_\eta$ stands for the Kolmogorov length scale, which is the length scale of the leaf level for the case of unity Schmidt number. The handling of variable Schmidt numbers is outlined in Section 4. After the grandparent node is selected, the swapping event is performed. For this purpose, a grandchild node is randomly selected from each of the left and right branches (children) of the grandparent node. The grandchildren of the grandparent node are then exchanged, or swapped along with their respective subtrees. Figure 1 shows this process at the selected parent node 0 with grandchildren 4 and 6. Note that nodes 3 and 5 could also have been selected as grandchildren. The exchange of fluid parcels taking place at the leaf level, the only physically relevant level of the tree, and the only level of the tree which is computationally stored, is an abstraction for the scale-reduction and advective rearrangement of fluid parcels in real turbulent mixing. Fluid properties stored at parcels located at the leaf level, undergo local modifications in their scalar gradients constructed from the discrete fluid properties stored at the leaf level. Considering one velocity component as a scalar, this would be the model analogy of increased strain due to turbulent advection. This complies with a local wavenumber increase, as in Kolmogorov turbulence (Kerstein, 2013).
The example in Figure 1 shows a swap involving grandchildren at tree levels higher than the leaf level. Another situation occurs when the grandparent node 1 is selected, and, as an example, grandchildren nodes 8 and 9 are selected accordingly. The swapping event takes place at the leaf level, which corresponds to the smallest represented physical length scale. The parcel swapping

Tab. 2: Length and time scales of the binary tree used in HiPS.

| level | length scale | time scale |
|---|---|---|
| 0 | $L_0$ | $\tau_0$ |
| 1 | $L_0/2$ | $\tau_0/2^{2/3}$ |
| 2 | $L_0/4$ | $\tau_0/4^{2/3}$ |
| i | $L_0/2^i$ | $\tau_0/(2^i)^{2/3}$ |
| ... | ... | ... |
| $n-1$ | $L_0/2^{n-1}$ | $\tau_0/(2^{n-1})^{2/3}$ |

changes the proximity within a fluid parcel pair and causes a subsequent mixing process. This is the case in Figure 2. A similar swapping event could occur if node 2 were selected as the grandparent node.
The mixing process, which is termed mixing event, is represented by intermixing the contents of two adjacent fluid parcels (constituting a node-joined pair). Mixing events can be implemented either instantaneously or at rates consistent with the prevailing diffusion time scales. Instantaneous mixing is a particularly efficient way to perform mixing. In the example in Figure 2, an instantaneous mixing event would result in the scalar values of the adjacent parcels being replaced with the mean of the two parcels ($\frac{\phi_0+\phi_2}{2}$ for the left sub-tree of grandparent node 1 and $\frac{\phi_1+\phi_3}{2}$ for the right sub-tree of grandparent node 1).
One salient feature of HiPS is that the mixing process itself is not restricted to a specific operation or rule. The mixing process could also be adapted to implement any existing mixing rule, e.g., IEM, without loss of generality. In Kerstein (2013, 2014), and in the example presented in Figure 2, the mixing rule is equivalent to Curl's model. Thus, HiPS effectively integrates all features of Curl's model. Considering the constrains and desired properties for a good mixing model in Table 1, HiPS already satisfies criterion (I) and (II). Additionally, the underlying binary tree structure in HiPS allows a dependence of the mixing rate on the scalar length scales (VI), see Table 2 and (Kerstein, 2013). Another important advantage of HiPS is the fact that the mixing is local in composition space (V). The size of the tree is determined by the Reynolds number, see Equation 4 and Starick and Schmidt (2019). Criterion (VII) is therefore also partially satisfied. The current HiPS formulation can be extended by a handling of variable Schmidt numbers, as described in Section 4. This enables HiPS to incorporate differential diffusion and consider criterion (VIII). This is a major advantage of the model and a significant difference to the common mixing models, see Starick and Schmidt (2019). In Subsection 3.4, preliminary results for the temporal evolution of the inert-scalar PDF are shown, which is crucial for the evaluation for criterion (III).
From a computational point of view, the binary tree representation of the model allows an efficient way to treat parcel advection. That is, parcel movements can be simply represented by a bit shift in an index array pointing to locations in the various variable arrays (Kerstein, 2013). The efficient implementation of HiPS and its physical basis opens the door for the evaluation of higher order statistics in scalar turbulence in large parameter investigations, e.g., the skewness and hyperskewness of the scalar derivative required in order to discuss anomalous behavior of scalar structure functions (Sreenivasan, 2019).

## 3 Results

Passive scalar mixing represents a simple but equally important case for comparison. In Figure 3, the temporal evolution of a passive scalar mixing HiPS simulation is shown. The binary tree used for this simulation spans 12 levels. The plot illustrates the mixture fraction of the scalar against the fluid parcel indices. The scalar profile is initialized with a step function. All scalar values of the parcels in the left sub-tree of root node are set to the value of 0 and all scalar values of the parcels in the right sub-tree of the root node 0 are set to the value of 1. This is indicated in Figure 3 by the blue solid line (Initial). At a later time ($5\tau_0$), the effects of the swapping and mixing events on the mixture fraction can be seen. After sufficiently long time ($> 15\tau_0$), the flow is more mixed (approaching the final mean value of 0.5) and only smaller fluctuations can be seen compared to the orange curve ($5\tau_0$). After a time of $\approx 30\tau_0$ (not shown here), everything is completely mixed and fluctuations can no longer be seen.

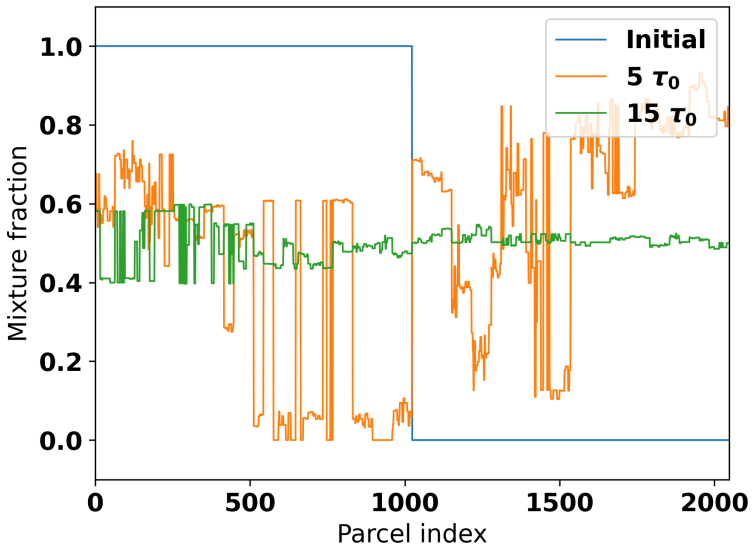


Fig. 3: Illustration of passive scalar mixing in HiPS. The mixture fraction of the passive scalar is given initially and at two later times.

The following Subsections (3.1, 3.2 and 3.3) show and discuss preliminary results of a passive scalar mixing HiPS simulation. For all shown results, the same settings were used. The binary tree spans 16 levels with an associated Reynolds numbers of approximately one million. The scalar profile is initialized with a step function profile. All scalar values in the parcels at the left-hand sub-tree of the root node 0 are set to the value of 0 and all scalar values in the parcels at the right-hand sub-tree of the the root node 0 are set to the value of 1. The simulation considers turbulent forcing, which means that each time there is a top-level

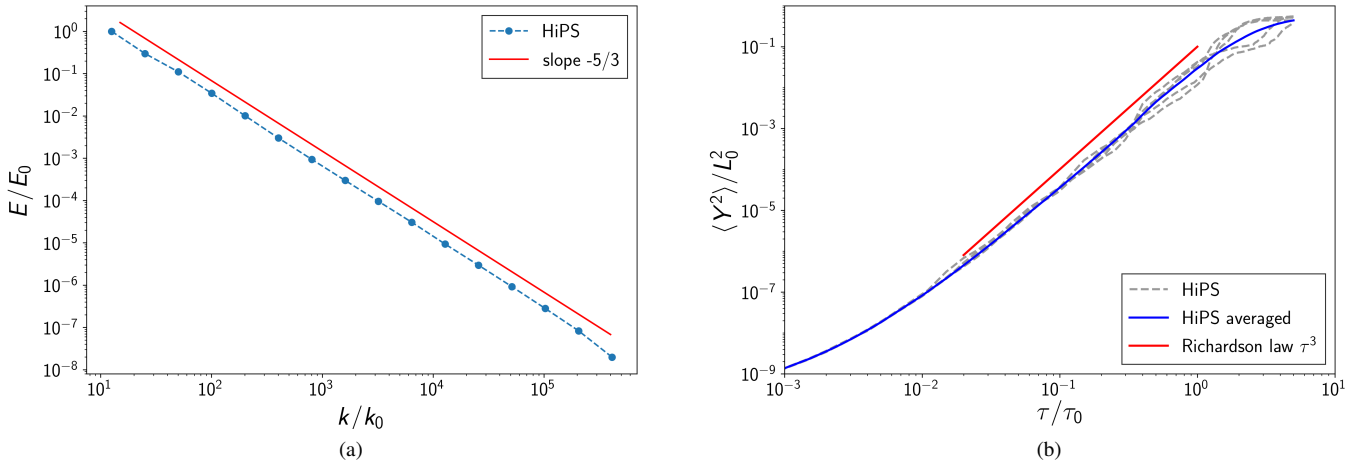


Fig. 4: (a) Scalar power spectrum of a passive scalar mixing HiPS simulation with forced turbulence using a step function initial condition (scalar value of 1 in all parcels at left-hand sub-tree and scalar value of 0 in all parcels of right-hand sub-tree). The dotted line shows the scalar power spectrum averaged over a time range of $100\tau_0$. The solid red line demonstrates -5/3 slope for comparison. (b) Mean square displacement of a passive scalar mixing HiPS simulation with forced turbulence. The blue solid line shows ensemble averaged HiPS results for the mean square displacement with a sample size of 100 realizations. The 5 gray dotted lines mark the mean square displacement for 5 independent HiPS realizations. The red solid line shows the Richardson-scaling law of $\tau^3$ for comparison.

swapping event (swapping at grandparent node 0), a constant is added to the parcels in a given half of the domain so that their average is either 0 (left half) or 1 (right half). This turbulent forcing procedure doesn't change the overall mean and leaves the statistical variance of the sub-trees unaffected.

### 3.1 Scalar spectrum

In HiPS, the generation of a scalar spectrum is not obvious and is reviewed in Kerstein (2013). The tree structure induces a reduction of the length scales $L_i$ with increasing levels $i$ of the tree. Every step towards to the base of the tree results in an increase in the implied wavenumber $k_i = \frac{2\pi}{L_i}$. The mean variance across all sub-trees $2^i$ at a given level $i$ is defined as $var_i\phi$, where $\phi$ denotes the scalar field. The HiPS analog of a scalar power spectrum can be calculated by $E(k) \sim \frac{1}{k_i}(var_{i-1}\phi - var_i\phi)$. In this context, $E(k)$ can be interpreted as scalar energy.
In Figure 4a, the scalar power spectrum for passive scalar mixing with forced turbulence is shown. The dotted line marks the HiPS generated scalar power spectrum averaged over a time range of $100\tau_0$. The markers indicate the scalar $E(k)$ and the associated wavenumber $k_i$ for the levels of the tree. A normalization with the maximum scalar energy $E_0$ and maximum wavenumber $k_0$ is carried out. For comparison purposes, the red line indicates a slope of -5/3 which represents the fundamental scaling relation of Kolmogorov turbulence of $E(k) \sim k^{-5/3}$ in the inertial range. Figure 4a demonstrates that HiPS can reproduce this scaling behavior that is one of the core principles of the model.

### 3.2 Richardson dispersion

The dispersion of particles under the influence of turbulence still poses challenges in fluid dynamics (Elsinga et al., 2022). The dispersion describes how far initially adjacent particles are spatially separated from each other. Predictions for the dispersion under the influence of turbulence of particle pairs dates back to 1926 when Richardson (1926) published an empirical approach where the mean square dispersion grows in time as $\tau^3$.
In Figure 4b, the mean square displacement $\langle Y^2\rangle$ versus time $\tau$ is presented for passive scalar HiPS simulations. A simple procedure to determine the dispersion $Y$ of a parcel pair in HiPS is based on the length scale of the nearest shared parent. As in Figure 2 shown, for the fluid parcels at nodes 9 and 10, the nearest shared parent has a length scale of $L_2$ (length scale of level 2). Similar to this procedure, for the fluid parcels at nodes 8 and 10, the nearest shared parent has a length scale of $L_1$ and for the fluid parcels at nodes 7 and 13, the nearest shared parent has length scale $L_0$.
In Figure 4b, the mean square displacement $\langle Y^2\rangle$ is normalized by the square of the integral length scale $L_0$ and the time $\tau$ is normalized by the integral time scale $\tau_0$. The blue solid line shows ensemble averaged HiPS results for the mean square displacement with a sample size of 100 realizations. The 5 gray dotted lines mark the mean square displacement for 5 different and independent HiPS realizations. The deviations of the gray lines from the blue line shows the randomness of the swapping events which is also influencing the mean square displacement. The red solid lines shows the Richardson-scaling law of $\tau^3$ for comparison. It can be seen after a sufficiently long time the mean square displacement follows Richardsons dispersion law. Batchelor (1950) predicted that the mean square displacement for times shorter than a characteristic timescale grows as $\tau^2$. The characteristic timescale depends on the initial separation of the considered parcel pair. An investigation of the $\tau^2$-scaling in HiPS is planned in the near future. A finer temporal resolution of the initial phase and a wider range of length and time scales may be necessary for a detailed consideration of the Batchelor scaling. All in all, it is remarkable that such a simple and efficient mixing model is able to

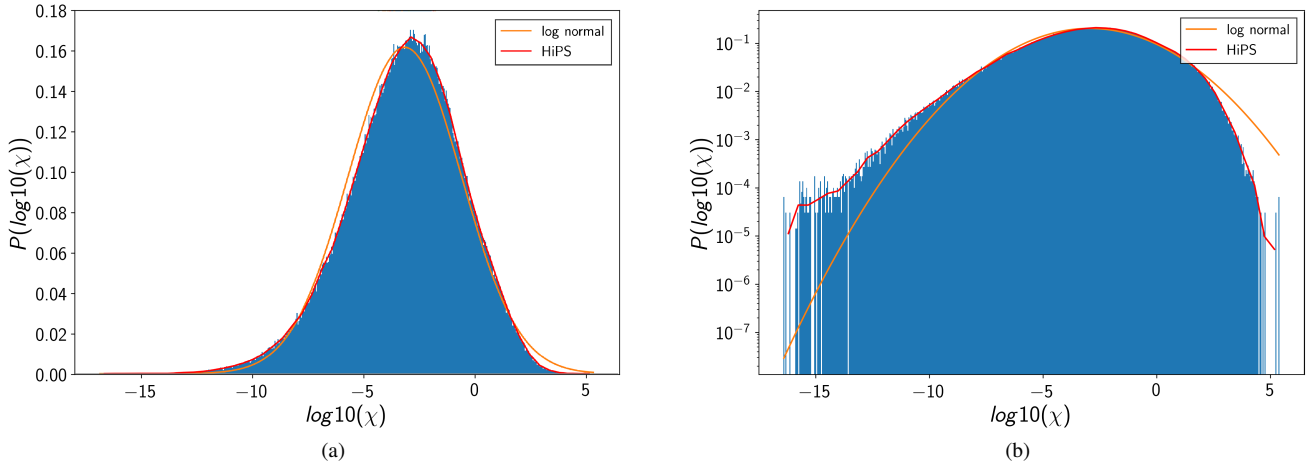


(a) (b)

Fig. 5: (a) Probability Density Function (PDF) of the logarithmic scalar dissipation rate for a passive scalar mixing simulation in HiPS with a linear y-axis. The orange curve presents a log-normal distribution with the mean and standard deviation calculated from the HiPS results. (b) PDF of the logarithmic scalar dissipation rate for a passive scalar mixing simulation in HiPS with a logarithmic y-axis.

reproduce the Richardson dispersion law for the mean square displacement.

### 3.3 Scalar dissipation rate

The mixing of scalars in turbulent flows is a very interesting problem which provides a fundamental understanding of the basic processes involved. A key quantity in turbulent mixing that directly indicates the rate of decay of scalar fluctuations is the scalar dissipation rate $\chi$.
The scalar dissipation rate is defined by Fox (2003),

$$\chi = \left\langle 2\Gamma \frac{\partial \phi'}{\partial x_i} \frac{\partial \phi'}{\partial x_i} \right\rangle \tag{5}$$

In Equation 5, $\Gamma$ is the diffusion coefficient of the scalar and $\frac{\partial \phi'}{\partial x_i}$ is the fluctuating scalar gradient. In this context, $\phi$ is often taken as the mixture fraction. Since HiPS uses fluid parcels with proximities defined by the binary tree structure, a suitable formulation of the scalar dissipation rate in HiPS is needed. The definition of the scalar dissipation rate in HiPS is based on a similar scaling approach as in Equation 2. For the diffusion coefficient $\Gamma \sim L^2/\tau$. The analogy to the fluctuating scalar gradient is given by the changes of the scalar field by the occurrence of swapping events. $\Delta\phi$ is computed by $\Delta\phi = \phi^{**} - \phi^{*}$. $\phi^{**}$ is the mixture fraction of the scalar before a swapping event and $\phi^{*}$ is the mixture fraction of the scalar after a swapping event.

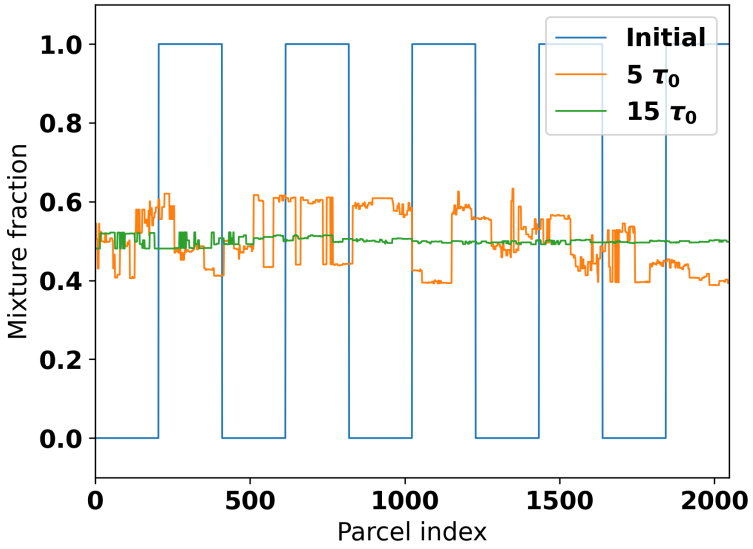


Fig. 6: Illustration of one passive scalar HiPS mixing simulation. The mixture fraction of the passive scalar is given at the beginning (Initial) and at two different times along the fluid parcels.

This results in following relationship for the definition of the scalar dissipation rate in HiPS,

$$\chi = 2\frac{(\Delta\phi)^2}{\tau_{mix}}. \tag{6}$$

In Equation 6, $\tau_{mix}$ is the time since the last occurrence of a mixing process at the fluid parcel.
In Figure 5a and 5b, the PDF of the log of the scalar dissipation rate is shown. For comparison purposes, a normal distribution with the mean and standard deviation calculated from the HiPS results is illustrated. Figures 5a and 5b indicates that, beside the far end tails, the commonly accepted log-normal distribution of the scalar dissipation rate $\chi$ is preserved. Additionally, HiPS exhibits a negative skewness in Figure 5b, which is also seen in experiments and DNS (Watanabe and Gotoh, 2004).

### 3.4 Inert-scalar PDF

The temporal evolution of the scalar PDF in passive scalar mixing is an crucial evaluation criterion. The scalar dissipation rate strongly depends on the initial condition and thus on the initial scalar length scale distribution. As a result, the temporal evolution of the inert-scalar PDF also depends on the initial condition. As known from DNS (Eswaran and Pope, 1988), the PDF of inert scalars relaxes to a multi-variate Gaussian form in homogeneous turbulence for arbitrary initial conditions. This fact is also used for the evaluation of a mixing model, see criteria (III) in Table 1.
The evaluation of the temporal evolution of the scalar PDF can also be done with HiPS. In Figure 7, preliminary results for the inert-scalar PDF at different times for a 12 level binary HiPS tree are shown. The results are ensemble-averaged over a sample size of 3000. In contrast to the results shown so far, the initial condition is different here. In Figure 6, the initial condition and the temporal evolution of the mixture fraction along the fluid parcels is presented. The initial condition is based on a zigzag profile. Compared to a one step profile (see Figure 3), the initial length scales are smaller. The initial PDF has only the values of 0 and 1. With increasing time, the mixing progress advances and accumulates values around the mean of 0.5. A qualitative comparison of the shape of the PDF at $7\tau_0$ gives the impression that it has a Gaussian form. However, this requires further investigations before this can be confirmed. A final decision on the fulfillment of criterion (III) for HiPS in Table 1 cannot be made. However, the preliminary results are promising. With further increasing time, the PDF is concentrated close to the mean of 0.5 until no fluctuations around the mean can be detected (delta peak at 0.5 not shown here).

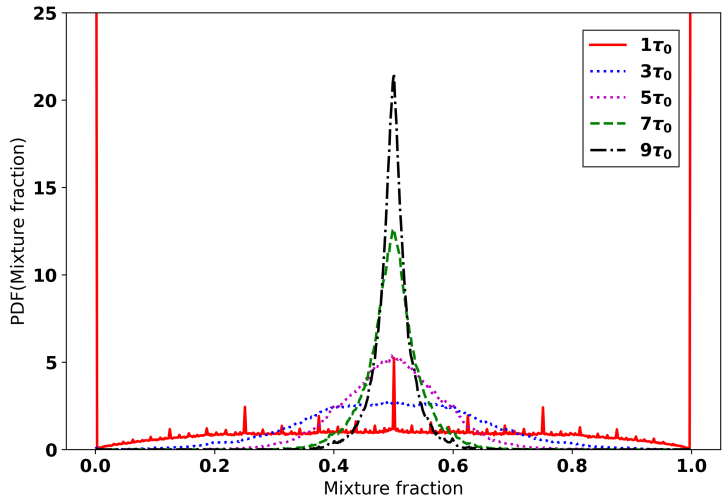


Fig. 7: Ensemble averaged inert-scalar PDF from 3000 stand-alone HiPS simulations at 5 different times.

## 4 Incorporation of differential diffusion

In the current HiPS formulation, only unity Schmidt number passive scalars can be considered. This means that the Kolmogorov and Batchelor length scales are located on the same level. Arbitrary Schmidt number effects can be incorporated in the model by modifying the micromixing and swapping procedure, effectively allowing the creation of additional and intermediate levels in the binary tree. For the case of $Sc < 1$, the scalar has a very high diffusivity and the Batchelor length scale is larger than the Kolmogorov length scale. In this case, the mixing process can take place only on levels above the leaf level (above the Kolmogorov scale).
The contrary is the case if $Sc > 1$. The diffusivity of the scalar is low and the Batchelor length scale is smaller than the Kolmogorov length scale. For the binary tree representation, this implies the existence of additional tree levels below the existing leaf level, which are turbulently advected, but only by swapping events with grandchildren on Kolmogorov or larger length scales. This implies that the nodes at these levels may be swapped as a consequence of a swapping event on upper tree nodes, but they can not be selected as children nodes themselves. Mixing processes, nonetheless, given by the set of mixing rules implied in the model, may still take place at these nodes below the leaf level.

The model extension for the treatment of variable Schmidt numbers opens the door for the investigation of differential diffusion effects, i.e., simultaneous mixing of scalars with different Schmidt numbers. Differential diffusion effects could be simulated in practice by specifying different mixing rules for each scalar in the binary tree. This allows investigation of multi-parcel correlations and scaling laws at very large or small Reynolds and Schmidt numbers.

## 5 Summary

HiPS is a novel, computationally efficient and physics-based mixing model which at the same time fulfills constraints for good mixing models and several desirable properties of mixing models like locality of mixing in composition space, dependence of the mixing rate on scalar length scales and the incorporation of parametric dependencies such as Reynolds and Schmidt number dependencies. Additionally, the possibility to consider a large range of scales while being computationally tractable is a significant advantage.

The results show noticeable agreement with known theories in passive scalar mixing. Given the simplicity of the model, a reproduction of the Richardson dispersion in passive scalar mixing and the preservation of a log-normal distribution of the PDF of the scalar dissipation rate are remarkable results. The extension to variable Schmidt numbers as described in the previous section is a necessary next step in the stand-alone HiPS formulation to investigate multi-parcel correlations as well as scaling laws at very large or small Reynolds and Schmidt numbers.

It is noted that HiPS has also been formulated as a turbulence model in Kerstein (2014, 2021), by means of the incorporation of momentum equations, and the use of a stochastic sampling procedure for swapping events analogous to the implementation of eddy events in the One-Dimensional Turbulence model (Kerstein, 1999). A future application of HiPS could be the coupling with LES or RANS in a top-down or bottom-up approach, or by means of a sub-grid mixing model in PDF transport methods.

## Acknowlegement

This work was supported by BTU Graduate Research School (Conference Travel Grant).

## References

G. K. Batchelor. The application of the similarity theory of turbulence to atmospheric diffusion. *Quarterly Journal of the Royal Meteorological Society*, 76(328):133–146, 1950. doi: https://doi.org/10.1002/qj.49707632804.

R. L. Curl. Dispersed phase mixing: I. Theory and effects in simple reactors. *AIChE J.*, 9:175–181, 1963. doi: https://doi.org/10.1002/aic.690090207.

C. Dopazo. Relaxation of initial probability density functions in the turbulent convection of scalar fields. *The Physics of Fluids*, 22 (1):20–30, 1979. doi: 10.1063/1.862431.

C. Dopazo. Recent developments in pdf methods. *Turbulent reacting flows*, 375:474, 1994.

C. Dopazo and E. E. O'Brien. An approach to the autoignition of a turbulent mixture. *Acta Astronaut.*, 1(9):1239 – 1266, 1974. ISSN 0094-5765. doi: https://doi.org/10.1016/0094-5765(74)90050-2.

G. E. Elsinga, T. Ishihara, and J. C. R. Hunt. Non-local dispersion and the reassessment of richardson's t3-scaling law. *Journal of Fluid Mechanics*, 932:A17, 2022. doi: 10.1017/jfm.2021.989.

V. Eswaran and S. B. Pope. Direct numerical simulations of the turbulent mixing of a passive scalar. *The Physics of Fluids*, 31(3): 506–520, 1988. doi: 10.1063/1.866832.

J. H. Ferziger, M. Perić, and R. L. Street. *Computational Methods for Fluid Dynamics*. Springer Cham, 2020. ISBN 978-3-319-99691-2. doi: https://doi.org/10.1007/978-3-319-99693-6.

R. O. Fox. *Computational models for turbulent reacting flows*. Cambridge university press, 2003. doi: 10.1017/CBO9780511610103.

C. Glawe, J. A. Medina Méndez, and H. Schmidt. IMEX based multi-scale time advancement in ODTLES. *J. Appl. Math. Mech. (Engl. Transl.)*, 98(11):1907–1923, 2018. doi: 10.1002/zamm.201800098.

J. Janicka, W. Kolbe, and W. Kollmann. Closure of the transport equation for the probability density function of turbulent scalar fields. *J. Non-Equilib. Thermodyn.*, 4:47–66, 1979. doi: doi:10.1515/jnet.1979.4.1.47.

A. R. Kerstein. One-dimensional turbulence: model formulation and application to homogeneous turbulence, shear flows, and buoyant stratified flows. *J. Fluid Mech.*, 392:277–334, aug 1999. doi: 10.1017/S0022112099005376.

A. R. Kerstein. Hierarchical parcel-swapping representation of turbulent mixing. Part 1. Formulation and scaling properties. *J. Stat. Phys.*, 153(1):142–161, 2013. doi: https://doi.org/10.1007/s10955-013-0811-z.

A. R. Kerstein. Hierarchical parcel-swapping representation of turbulent mixing. Part 2. Application to channel flow. *J. Fluid Mech.*, 750:421–463, 2014. doi: 10.1017/jfm.2014.276.

A. R. Kerstein. Hierarchical parcel-swapping representation of turbulent mixing. III. Origins of correlation patterns observed in turbulent boundary layers. *Phys. Rev. Fluids*, 6:044611, 2021. doi: 10.1103/PhysRevFluids.6.044611.

A. N. Kolmogorov. The local structure of turbulence in incompressible viscous fluid for very large Reynolds numbers. *Proc. R. Soc. London, Ser. A*, 434(1890):9–13, 1991. doi: 10.1098/rspa.1991.0075.

D. Livescu, A. G. Nouri, F. Battaglia, and P. Givi. *Modeling and Simulation of Turbulent Mixing and Reaction For Power, Energy and Flight: For Power, Energy and Flight*. 01 2020. ISBN 978-981-15-2642-8. doi: 10.1007/978-981-15-2643-5.

A. M. Obukhov. Kolmogorov flow and laboratory simulation of it. *Russian Mathematical Surveys*, 38(4):113–126, 1983. doi: 10.1070/rm1983v038n04abeh004207.

S. B. Pope. PDF methods for turbulent reactive flows. *Prog. Energy Combust. Sci.*, 11(2):119 – 192, 1985. ISSN 0360-1285. doi: https://doi.org/10.1016/0360-1285(85)90002-4.

S. B. Pope. *Turbulent Flows*. Cambridge University Press, 11th edition, 2011. ISBN 9781139643351.

L. F. Richardson. Atmospheric diffusion shown on a distance-neighbour graph. *Proceedings of the Royal Society of London. Series A, Containing Papers of a Mathematical and Physical Character*, 110(756):709–737, 1926. doi: https://doi.org/10.1098/rspa.1926.0043 Abstract.

B. I. Shraiman and E. D. Siggia. Scalar turbulence. *Nature*, 405(6787):639 – 646, 2000. doi: https://doi.org/10.1038/35015000.

K. R. Sreenivasan. Turbulent mixing: A perspective. *Proc. Natl. Acad. Sci.*, 116(37):18175–18183, 2019. doi: 10.1073/pnas.1800463115.

T. Starick and H. Schmidt. Hierarchical parcel-swapping: An efficient mixing model for turbulent reactive flows. *PAMM*, 19, 2019. doi: 10.1002/pamm.201900492.

S. Subramaniam and S. B. Pope. A mixing model for turbulent reactive flows based on Euclidean minimum spanning trees. *Combust. Flame*, 115(4):487 – 514, 1998. ISSN 0010-2180. doi: https://doi.org/10.1016/S0010-2180(98)00023-6.

K. Tsai and R. O. Fox. Modeling the scalar dissipation rate for a turbulent series-parallel reaction. *Chem. Eng. Sci.*, 51(10):1929 – 1938, 1996. doi: https://doi.org/10.1016/0009-2509(96)00050-4.

E. Villermaux. Mixing Versus Stirring. *Annu. Rev. Fluid Mech.*, 51(1):245–273, 2019. doi: 10.1146/annurev-fluid-010518-040306.

J. Villermaux and J. C. Devillon. Représentation de la coalescence et de la redispersion des domaines de ségrégation dans un fluide par un modèle d'interaction phénoménologique. *Chem. React. Eng., Proc. Int. Symp., 2nd*, 2:1–13, 1972.

T. Watanabe and T. Gotoh. Statistics of a passive scalar in homogeneous turbulence. *New J. Phys.*, 6:1–37, 2004. doi: 10.1088/1367-2630/6/1/040.